

Theoretical investigation of cyclooxygenase inhibition property of several non-steroidal anti-inflammatory drugs by density functional theory calculations and molecular docking studies

Atena Najdian¹, Amirhossein Sakhteman^{1,*}, Maryam Mortazavi¹, Hossein Sadeghpour¹, Massoud Amanlou²

¹Department of Medicinal Chemistry, School of Pharmacy, Shiraz University of Medical Sciences, Shiraz, Iran.

²Department of Medicinal Chemistry, Faculty of Pharmacy and Drug Design & Development Research Center, Tehran University of Medical Sciences, Tehran, Iran.

Abstract

Understanding the geometry and electronic properties of non-steroidal anti-inflammatory drugs (NSAIDs) and the nature of their interactions with human cyclooxygenase-2 (COX-2) is important in the development and design of novel NSAIDs. In this paper, B3LYP/6-311++G (d,p) level of theory was applied to assess the acidity of NSAIDs in the gas phase. Subsequently, the role of intramolecular hydrogen bond on acidity of these compounds was confirmed by means of natural bond orbital (NBO) and quantum theory of atoms in molecules analyses (QTAIM). Furthermore, by applying the polarized continuum model (PCM) at the B3LYP/6-311++G(d,p) level, the pK_a value of NSAIDs in aqueous solution was calculated. The maximum error was found to be less than 0.1 pK_a unit in comparison with the experimental value. This protocol can be used as a tool to predict pK_a values of NSAIDs in future studies. In the last step, attempts have been made to generate a functional model of the structure of human COX-2 enzyme by means of homology modeling to gain more insight into the nature of interactions between NSAIDs and the active site of this COX-2 enzyme by docking studies. In addition, a mean binding energy for each drug was estimated based on its ionization ratio.

Keywords: Cyclooxygenase-2 inhibitors, DFT calculations, Docking studies, Homology modeling, pK_a .

1. Introduction

Non-steroidal anti-inflammatory drugs (NSAIDs) constitute a noteworthy class of medications for the alleviation of pain, inflammation, and fever. NSAIDs exert their anti-inflammatory effect through the inhibition of prostaglandins (PG) synthesis, and more specifically the inhibition of cyclooxygenase enzymes, COX-1 and COX-2 (1). Although both enzymes are associated with inflammation, the former is considered to be constitutive, while the latter is considered as an inducible isoform. Based on the

described discovery, it was stated that inhibition of COX-1 results in an anti-inflammatory action as well as gastric irritation, whereas inhibition of COX-2 results in therapeutic effects (2).

The other roles of COX-2 inhibitors have been widely explored. For illustrative purposes, the antitumor activity and neurodegenerative diseases like Alzheimer's disease could potentially be relieved with NSAIDs (3-5). In addition, the antitumor activity of NSAIDs has been attributed to a synergism effect with antitumor drugs in clinical use (6).

NSAIDs can be classified based on their chemical structures into different type of families such as salicylates (Aspirin), propionic acid derivatives (Naproxen, Fenoprofen, Ketoprofen,

Corresponding Author: Amirhossein Sakhteman, Department of Medicinal Chemistry, School of Pharmacy, Shiraz University of Medical Sciences, Shiraz, Iran.

Email: asakhteman@sums.ac.ir

Flurbiprofen), anthranilic acid derivatives (Meclufenamic acid, Flufenamic acid, Tolfenamic acid), and acetic acid derivatives (diclofenac) (7). Naproxen demonstrates favorable anti-inflammatory, analgesic, and antipyretic property (8) and is utilized in inflammation conditions like rheumatoid arthritis, spondylitis, and osteoarthritis (9). Moreover, Tolfenamic acid was shown to be anti-pyretic, antirheumatoid, and anti-inflammatory. It is also administered for veterinary intentions (10). The importance of NSAIDs has led to numerous investigations by several authors. For instance, Kely Ferreira de Souza *et al* (11) have reported that in non-polar solvents the enol form of piroxicam leads to increase fluorescence. Their B3LYP/CEP-31G(d, p) level of calculations raise the importance of the hydrogen bonds in the stabilization of this tautomer. Hence, this enol form tends to show greater rigidity and planarity than the keto tautomer, making it more suitable to be involved in radiative processes (11). Furthermore, in another research, a density functional theory (DFT) study of allylic hydroxylation and double bond epoxidation in a model reaction have accomplished helped to gain more information about the factors that affect the regioselectivity of oxidation by cytochrome P450 (12). The mechanism for binding of different selective NSAIDs like celecoxib and rofecoxib towards COX-2 has been investigated (13) by using a wide range of theoretical techniques, including molecular dynamics and free energy calculations.

In physiological conditions, NSAIDs are present at different ionic states based on their pK_a values. Different docking results could be, therefore, expected for ionized or unionized states of the structures. By considering the ionization ratio of the structures, more accurate docking energy values would be estimated. For this purpose, it is of great importance to develop a valid method in order to calculate the pK_a values of NSAIDs.

On the basis of the preceding considerations, a preliminary investigation on the geometry, electronic properties, and acidity of NSAIDs was done. The human structure of COX-2 was thereafter generated by means of homology modeling. Docking simulations of some representative NSAIDs were subsequently performed

with the modeled structure of COX-2. Finally, the interactions between these optimized drugs and COX-2 enzyme system was investigated in order to shed light on the nature of these interactions. Binding mode of the ligands at different ionization states was explored, and a mean binding energy for each ligand was estimated.

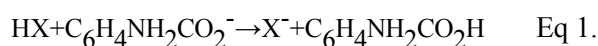
2. Methods

2.1. Density Functional Theory Study

The initial configurations of the studied NSAIDs and their corresponding conjugate bases were determined by Spartan 06 software (14). Thereafter, for the most stable conformers, geometry optimizations, and frequency calculations were totally carried out by the density functional theory (DFT) method applying Becke3 (B3) exchange and Lee, Yang, and Parr (LYP) correlation potentials (15, 16). The natural bond orbital (NBO) and quantum theory of atoms in molecules (QTAIM) analyses are shown to be very useful in portraying electron densities in different types of systems and in enlarging the concepts of H-bonds (17-19). NBO (20, 21) analysis was performed for the compounds of this study in order to obtain the natural charges by applying B3LYP/6-311++G (d, p) level. Moreover, B3LYP/6-311++G (d, p) level was used for quantum theory of atoms in molecules (QTAIM) analysis with AIM2000 package (22) in order to calculate the features of bond critical points (BCPs).

In case of solution phase, the solvation model requires an approximately much computational cost and is only suitable for a limited number of small molecule formulas. Among the suggested solvation models, polarized continuum model (PCM) is one of the most appropriate methods (23, 24). As a result, all geometrical optimizations that account for solvent effect, were carried out in water at the PCM/rB3LYP/6-311++G (d,p) level. Prediction of pK_a values in water was done using equation (1) where:

$$[\Delta G_{\text{rxn}}^{\circ}(\text{kcalmol}^{-1})]/1.364 = pK_a(\text{HX}) - pK_a(\text{C}_6\text{H}_4\text{NH}_2\text{CO}_2\text{H}) \text{ or } pK_a(\text{HX}) = pK_a(\text{C}_6\text{H}_4\text{NH}_2\text{CO}_2\text{H}) + [\Delta G_{\text{rxn}}^{\circ}(\text{kcalmol}^{-1})]/1.364 \quad (25)$$



In this reaction, HX is denouncing for NSAIDs and $C_7H_7NO_2$ was used as the reference molecule. (3-phenylpropanoic acid was the other reference used in this study.)

2.2. Docking study

2.2.1. Cox-2 modeling

The 3D structure of human cyclooxygenase (COX-2) was obtained by means of comparative homology modeling (26). Selection of the template was done using BLAST (Basic Local Alignment Search Toolbox) at NCBI server. ClustalX2 was thereafter used to generate the in-

put alignment required for modeller software 9v14 (27). The modeler python script was designed in such a way to include the co-crystal ligand of the template structure inside the output models. 100 models were accordingly generated using modeller9v14 (27), and the best model was selected based on the DOPE score energy value. The final best output model of modeller was subjected to PROCHECK server in order to calculate Ramachandran plot (28). The validated model was subsequently used in further docking studies.

2.2.2. Docking simulation

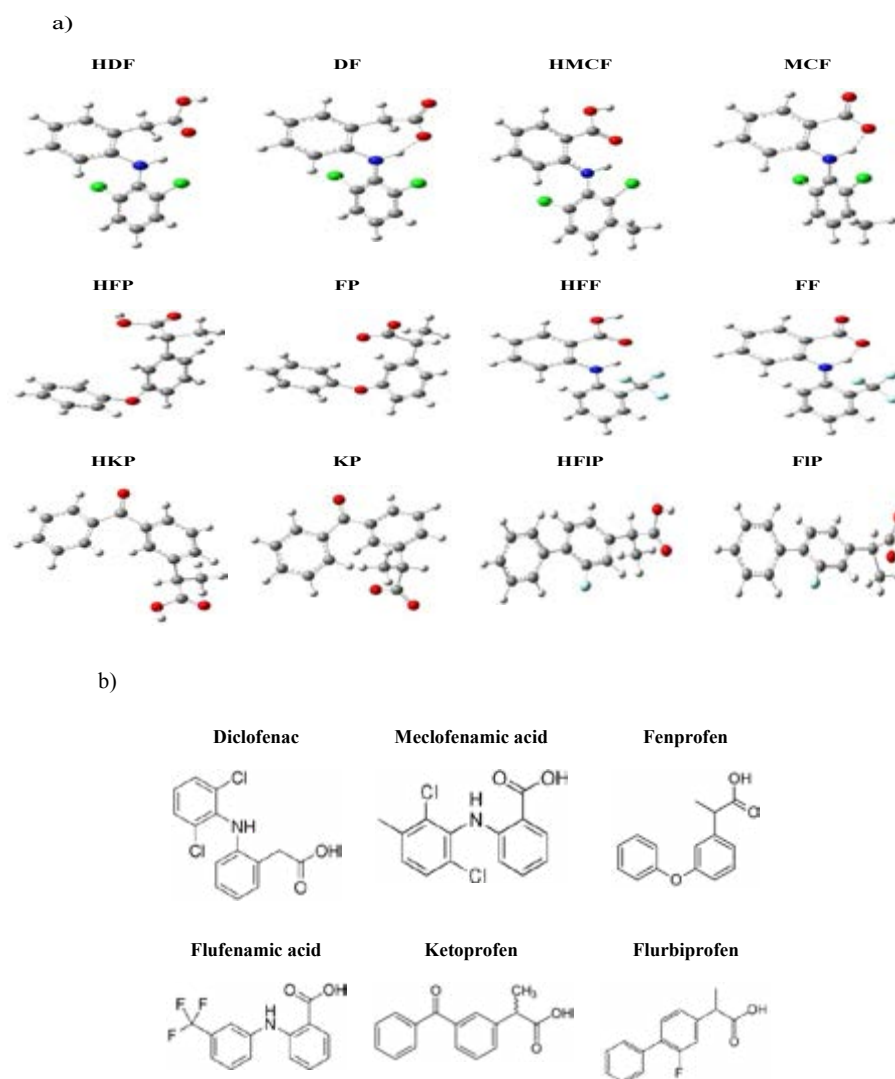


Figure 1. a) Optimized geometries using B3LYP/6-311++G (d, p) level of theory for the studied NSAIDs and their corresponding conjugate bases. (HDF=Diclofenac, DF=conjugate base of diclofenac, HMCF=Meclofenamic acid, MCF=conjugate base of meclofenamic acid, HFP=Fenpropfen, FP=conjugate base of fenpropfen, HFF=Flufenamic acid, FF=conjugate base of flufenamic acid, HKP=Ketoprofen, KP=conjugate base of ketoprofen, HFIP=Flurbiprofen, FIP= conjugate base of flurbiprofen) b) 2D representation of the NSAIDs used in this study.

Docking studies were carried out to provide insight into the interactions of NSAIDs at different ionization states with the active site of COX-2 enzyme. All docking simulations were performed by means of an in house batch scripts for automatic running of Autodock Vina 1.1.1 (29) in parallel using all system resources. The batch scripts were designed to facilitate the docking studies in an stepwise mode including ligand preparation, receptor preparation, conf.txt preparation, and finalization of docking runs. In all experiments, the genetic algorithm search method was used to find the best pose of each ligand in the active site of the target enzyme (30). The grid box dimension was considered as 25×25×25 Å and, the coordinates of the grid center were -40.486, -51.053, and -20.415, respectively. Random orientations of the conformations were generated after translating the center of the ligand to a specified position within the receptor active site. No attempt was made to minimize the ligand-receptor complex (rigid receptor docking). All visualization of protein ligand complexes was done using VMD software (31).

3. Results and Discussion

3.1. Acidity of NSAIDs in the gas phase

To find the most stable conformer of the studied compounds, various conformers with the potential energy surface at the interdependent energy range of 0-10 kcal/mol were determined. Merck molecular force field (MMFF) provided in Spartan 06 software was used for this purpose (14). Eventually, the obtained conformers were optimized at the B3LYP/6-311++G (d,p) level of theory. Their structures

with the lowest energy are exhibited in Figure. 1.

For HB at 298 K, the gas phase acidity is clearly described according to the following deprotonation process, $\text{HB} \rightarrow \text{H}^+ + \text{B}^-$. Enthalpy and the Gibbs free energy changes can be calculated as equation 2 (32):

$$\begin{aligned} \Delta H_{\text{acidity}} &= E(\text{HB}) - E(\text{B}^-) - E(\text{H}^+) + \Delta(\text{PV}) = E(\text{HB}) - E(\text{B}^-) \\ &\quad + E_{\text{vib}}(\text{HB}) - E_{\text{vib}}(\text{B}^-) - (5/2)RT \\ \Delta G_{\text{acidity}} &= \Delta H - T\Delta S \\ (\Delta S &= S(\text{HB}) - S(\text{B}^-) - S(\text{H}^+)) \end{aligned} \quad \text{Eq 2.}$$

Where $E(i)$, $E_{\text{vib}}(i)$ and $S(i)$, respectively, refer to the total energy, zero-point vibrational energy (ZPVE) also including the thermal vibrational corrections to the total energy for facilitation, and entropy of the species i . Both $(5/2)RT$ and $\Delta(\text{PV})$ terms include the translational energy of the proton.

The essential parameters for calculating the gas phase acidity of the mentioned compounds at 298 K are listed in Table 1. The formation of the intramolecular H-bond mostly within a six-member ring between oxygen lone pairs of the carboxylate moiety and the NH group, leads to a larger stabilization effect of the negative charge in some conjugate bases, shown in Figure 1, as a result yielding higher acidity. As seen in Table 1, there are two categories of weak organic acids among the studied NSAIDs based on their Gibbs energy changes. For instance, deprotonation process of HMCF is thermodynamically more favorable than HFP, because of intramolecular hydrogen bonding in the conjugate bases of the first compound. Strength of hydrogen bonding interactions is usually perceived by NBO and QTAIM

Table 1. B3LYP/6-311++G (d,p) thermochemical values for the studied NSAIDs and their corresponding conjugate bases.

Compound	E0+TC ^a (au)		$\Delta H_{\text{acidity}}^b$ (kcal/mol)	T $\Delta S_{\text{acidity}}^c$ (kcal/mol/K)	$\Delta G_{\text{acidity}}^d$ (kcal/mol)
	acid	anion			
HMCF	-1665.753898	-1665.233033	328.33	7.06	321.27
HDF	-1665.749569	-1665.228779	328.28	6.79	321.49
HFP	-805.663732	-805.132105	335.08	7.34	327.74
HFF	-1044.343256	-1043.822186	328.46	7.32	321.14
HFIP	-829.711948	-829.181133	334.57	7.36	327.21
HKP	-843.785527	-843.258851	331.97	7.22	324.75

^aTotal energy values (TC is thermal correction); ^bEnthalpy changes, ^cThe product of Temperature and Entropy Changes and ^dGibbs energy changes at 298 K.

analyses as will be discussed in the next sections.

3.2. Natural bond orbital (NBO) analysis

NBOs (20) provide the most accurate feasible (natural Lewis structure) picture of the wave function ψ . All the orbital details are mathematically chosen so as to encompass the highest possible percentage of the electron density. Hence, in the NBO analysis, the donor-acceptor (bond-antibond) interactions are taken into consideration by inspecting all plausible interactions between donor and acceptor NBOs. Stabilization energy $E^{(2)}$ relevant to the delocalization trend of electrons from donor to acceptor orbitals is computed via perturbation theory. Large stabilization energy $E^{(2)}$ between a donor bonding orbital and an acceptor orbital indicates an achievable strong interaction between them. The stabilization energy $E^{(2)}$, which associates with $i \rightarrow j$ delocalization between donor orbital (i) and acceptor orbital (j), is given by the equation 3:

$$E^{(2)} = \Delta E_{ij} = \Delta E_{CT} = -2 \frac{(i|\hat{F}|j)^2}{\epsilon_j - \epsilon_i} \quad \text{Eq 3.}$$

Where ϵ_i and ϵ_j are NBO orbital energies, and F is the Fock operator (33). The necessary NBO parameters are given in Tables 2 and 3 for each NSAIDs and its conjugate base. They were estimated from the natural bond orbital (NBO) analysis at B3LYP/6-311++G (d, p) level. The major stabilizing effect is because of the potent orbital interactions between the antibonding orbital of proton donor σ^*N-H and the lone pairs

of proton acceptor $lp(O)$. As a result, the charge is transferred from the lone pairs of oxygen to σ^* orbitals of N-H or C-H bond in all compounds. Two lone pairs of the oxygen atom have been participated in some compounds unequally because of their dissimilar orientation in regard to σ^* orbitals. As a case in point, in DF compound, the sum of stabilization energies (i.e., $E^{(2)}$) for $lp(O15) \rightarrow \sigma^*(H18-N17)$ is much larger than that of $lp(O15) \rightarrow \sigma^*(H19-N18)$ interaction in HDF. This indicates the stronger hydrogen bonding interaction in the conjugate base structure than its corresponding acid. Whereas in compounds like HFP and FP, the acceptor orbital of intramolecular hydrogen bond is C-H bond, so that their importance in stabilization of the geometries are negligible due to their much lower $E^{(2)}$ values. Also, values of transferred charge in donation and back donation processes, Δq_{CT} , have been calculated and given in Table 2 and Table 3. Comparative values of Δq_{CT} with $E^{(2)}$ for these compounds show that charge transfer energies have the same trend as stabilization energies. In all of the studied NSAIDs in Table 2 and Table 3, the highest values of $E^{(2)}$ and Δq_{CT} belong to the conjugate bases than their corresponded acids.

3.3. Atoms in molecule analysis of hydrogen bonds

The bond properties between each pair of atoms were systematically analyzed using quantum theory of atoms in molecules (QTAIM) (17). Based on topological parameters, a direct connection extracts by giving attention to the electron density, in addition to the geometries and binding energies. These parameters embody values

Table 2. The significant natural bond orbital parameters for the intramolecular hydrogen bonding interactions of the studied NSAIDs, calculated at the B3LYP/6-311++G(d,p) level of theory.

Compound	Charge transfer	$E^{(2)a}$ (kcal/mol)	$E_t^{(2)b}$ (kcal/mol)	Δq_{ct}^c	$\sum \Delta q_{ct}^d$
HDF	$n_{O15(1)} \rightarrow \sigma^*H19-N18$	1.47	5.64	0.0633	0.1962
	$n_{O15(2)} \rightarrow \sigma^*H19-N18$	4.17		0.1329	
HMCF	$n_{O12(1)} \rightarrow \sigma^*H16-N15$	2.71	10.25	0.0864	0.2657
	$n_{O12(2)} \rightarrow \sigma^*H16-N15$	7.54		0.1793	
HFF	$n_{O12(1)} \rightarrow \sigma^*H16-O15$	2.88	10.74	0.0899	0.2714
	$n_{O12(2)} \rightarrow \sigma^*H16-O15$	7.86		0.1815	

^aSecond-order perturbation stabilization energies; ^bTotal stabilization energies; ^cCharge transfer values; ^dThe sum of charge transfer values.

Table 3. The significant natural bond orbital parameters for the intramolecular hydrogen bonding interactions related to the conjugate bases of the studied NSAIDs calculated at the B3LYP/6-311++G(d, p) level of theory.

Compound	Charge transfer	$E^{(2)a}$	$E_t^{(2)b}$	$E_t^{(2)}_{CB} - E_t^{(2)}_{AC}^c$	Δq_{ct}^c	$\sum \Delta q_{ct}^d$
		(kcal/mol)	(kcal/mol)	(kcal/mol)		
DF	$n_{O15(1)} \rightarrow \sigma^*H18-N17$	7.75	46.66	41.02	0.1563	0.5781
	$n_{O15(2)} \rightarrow \sigma^*H18-N17$	38.91			0.4218	
MCF	$n_{O12(1)} \rightarrow \sigma^*H15-N14$	7.32	47.50	37.25	0.1515	0.5841
	$n_{O12(2)} \rightarrow \sigma^*H15-N14$	40.18			0.4326	
FF	$n_{O12(1)} \rightarrow \sigma^*H15-N14$	7.09	44.17	33.43	0.1487	0.5678
	$n_{O12(2)} \rightarrow \sigma^*H15-N14$	37.08			0.4191	
KP	$n_{O31(1)} \rightarrow \sigma^*H10-C7$	0.76	0.76	0.76	0.0466	0.0466
FP	$n_{O30(1)} \rightarrow \sigma^*H11-C3$	0.62	0.62	0.62	0.0430	0.0430
FIP	-	-	-	-	-	-

^aSecond-order perturbation stabilization energies; ^bTotal stabilization energies; ^cDifference of the conjugate base $E_t^{(2)}$ and its corresponding acid $E_t^{(2)}$; ^dCharge transfer values; ^eThe sum of charge transfer values.

of the electron density ($\rho(r)$) and the Laplacian ($\nabla^2 \rho(r)$) at the bond critical point (BCP). Accordingly, a negative value of $\nabla^2 \rho(r)$ at a BCP is related to the covalent nature of a bond, while ($\nabla^2 \rho(r) > 0$) implies “closed-shell-type” interaction as seen in ionic bonds, hydrogen interactions, and van der Waals molecules (34). The required parameters to expound the essence of intramolecular hydrogen bond obtained from QTAIM analysis are presented in Table 4 for all compounds.

A positive value of ($\nabla^2 \rho(r)$), at various BCPs of NH...OH and CH...OH intramolecular hydrogen bonds is given in Table 4 for each acid

and its conjugate base. It illustrates that these interactions are mainly electrostatic in nature. Moreover, the values of $\rho(r)$ at BCPs of NH...OH intramolecular hydrogen bonds are higher than CH...OH ones. As a rule, $\rho(r)$ larger than 0.20 au and less than 0.10 au are related to covalent bonding and a closed-shell interaction, respectively (35). From the values of electron density in Table 4, it can be again deduced that in both NSAIDs and conjugate bases, intramolecular hydrogen bonds are all closed-shell interactions in BCPs. Thus, the higher acidity of the first category of NSAIDs (i.e., HMCF) than the second one (i.e., HFP) has

Table 4. Bond critical point data from QTAIM analysis.

Compound	BCP	$\rho(r)^a$	$\nabla^2 \rho(r)^b$
		(e/au^3)	(e/au^5)
HDF	$n_{O15(1)} \rightarrow \sigma^*H19-N18$	0.019	0.069
DF	$n_{O15(1)} \rightarrow \sigma^*H18-N17$	0.063	0.140
HMCF	$n_{O12(1)} \rightarrow \sigma^*H16-N15$	0.032	0.120
MCF	$n_{O12(1)} \rightarrow \sigma^*H15-N14$	0.070	0.151
HFF	$n_{O12(1)} \rightarrow \sigma^*H16-O15$	0.032	0.119
FF	$n_{O12(2)} \rightarrow \sigma^*H15-N14$	0.066	0.149
KP	$n_{O31(1)} \rightarrow \sigma^*H10-C7$	0.010	0.032
FP	$n_{O30(1)} \rightarrow \sigma^*H11-C3$	0.008	0.025
FIP	$n_{O29(1)} \rightarrow \sigma^*H19-C16$	0.012	0.039

^aThe electron densities; ^bLaplacians of the electron densities.

Table 5. Theoretical pK_a values of the studied NSAIDs.

Compound	$\Delta G_{rxn}^{\circ a}$	$pK_a(\text{calc})^b$	$pK_a(\text{exp})$	ΔpK_a
HDF	3.17	4.46	4.50 ^[41]	-0.04
HFP	-0.19	4.52	4.50 ^[42]	0.02
HFF	2.51	3.98	3.90 ^[43]	0.08
HFIP	-0.42	4.35	4.33 ^[44]	0.02
HKP	0.14	4.76	4.80 ^[41]	-0.04
HMCF	1.91	3.54	3.64 ^[45]	-0.10

^aGibbs energy changes of equation (1) in kcal/mol. ^bThe pK_a values calculated using the equation (1) for the studied NSAIDs.

been again proved again by QTAIM analysis.

3.4. Acidity of NSAIDs in aqueous solution

Many drugs contain at least one acidic and/or basic functionality, whose the ionization state of these functional groups plays an important role in determining the physicochemical properties of the compound. At a particular pH, the acid dissociation value of a drug compound is obtained via Henderson–Hasselbach equation (equation 4) (36):

$$pH = pK_a + \log\left[\frac{\text{unprotonated form}}{\text{protonated form}}\right] \quad \text{Eq. 4.}$$

In perception of the behavior of drug compounds, the ionization constant is a powerful parameter. In biochemistry and pharmacology, the information about the pK_a values of ionizable groups in a protein plays an essential role for comprehension of its functional mechanism at the molecular level (37). Most NSAIDs are weak organic acids, with pK_a of 3–5. They are absorbed well from the stomach and intestinal mucosa. They are highly protein-bound in plasma, usually to albumin, so that their volume of distribution

typically approximates to the plasma volume (38). The measurement of pK_a may not be not straightforward and it leads to a significant experimental challenge. Experiments must be very carefully performed under standard conditions to ensure the validity of the results (39). For these such reasons, it is of enormous interest to develop computational methods for predicting the pK_a value of drugs.

Bases on the pervious explanation provided, the pK_a values of the studied NSAIDs were computed in this research. The reference molecules, 2-aminobenzoic acid (for meclufenamic acid, diclofenac and flufenamic acid) and 3-phenylpropionic acid (for fenoprofen, ketoprofen, flurbiprofen) were used for the calculation; since they are similar enough to the family type of each compound. The experimental pK_a value of the former is 2.14 and the latter is 4.66 (40). The calculated pK_a values (obtained by equation (1)) for NSAIDs are listed in Table 5. The correlation between experimental pK_a values of these compounds and their calculated pK_a is displayed in Figure. 2. As seen in Table 5, for all NSAIDs in this work, the results of the theoretical method is very close to the experimental

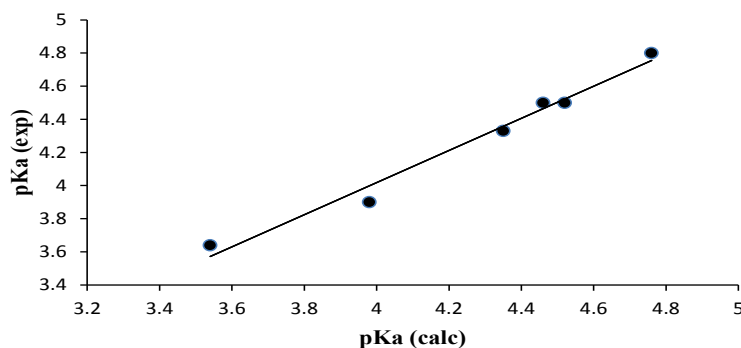


Figure 2. Experimental pK_a values versus calculated values for the studied NSAIDs ($R^2=0.9795$).

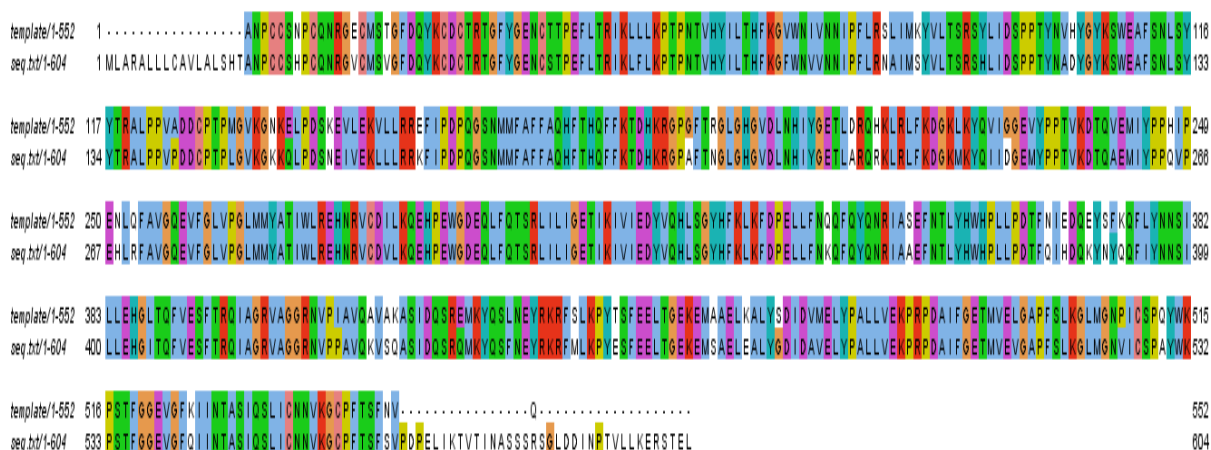


Figure 3. The alignment file used in homology modeling of human cyclooxygenase-2 (COX-2).

values. Comparison of these results demonstrates that a good correlation exists between the experimental results and the calculated values (Figure 2).

3.5. Docking study

The 3D structure of human cyclooxygenase-2 (Prostaglandin G/H synthase 2; Accession number: P35354) was generated based on the crystal structure of the homologue protein structure. The high resolution structure of mouse cyclooxygenase (3NT1; 1.74 Å) in complex with naproxen was selected by means of BLAST. The selected template was similar with 87% identity and 100% coverage to human COX-2 enzyme. The alignment file for the homology modeling step is depicted in Figure 3, and the conserved residues of both enzymes were aligned reasonably before modeling procedure. To keep the natural state of the active site of human enzyme, naproxen was also included in the output models. As described, the structure of the model was verified using Ramachandran plot. As seen in Figure 4, more than 92% of the

residues were in the most allowed regions. Some residues including His16 and Glu58 were not in the favored regions. Not more computational work has been done for these residues, since they were not taking role in the binding of the ligands. This verifies that the obtained model is in accordance with the folding, as anticipated for the natural protein structures. The proposed model was therefore a suitable structure to be used in docking studies. Ionization states of the residues were also corrected at physiological pH with respect to their isoelectric constants. Based on equation 4, the ratio of unprotonated form of the studied NSAIDs to their protonated form was computed in physiological pH by considering their calculated pK_a values. The result of this computation is summarized in Table 6. As demonstrated in Table 6, the dominate form of these drugs in physiologic pH is their unprotonated form. Therefore, in Binding Energy_{mean} value the contribution of this form is much greater than the protonated form. However, the ionization ratio is needed to correct the binding energy for

Table 6. The log [(unprotonated form/protonated form)], Binding Energy_{acid} (kcal/mol), Binding Energy_{anion} (kcal/mol) and Binding Energy_{mean} (kcal/mol) of the NSAIDs at 310 K and in pH=7.4.

Compound	The log[(unprotonated form/protonated form)]	BE _{acid}	BE _{anion}	BE _{mean}
HMCF	3.86	-7.2	-7.4	-7.39997
HDF	2.94	-6.8	-7.0	-6.99977
HFP	2.88	-8.4	-8.3	-8.30013
HFF	3.42	-7.3	-7.7	-7.69985
HFIP	3.05	-8.5	-8.7	-8.69982
HKP	2.64	-7.9	-8.4	-8.39886

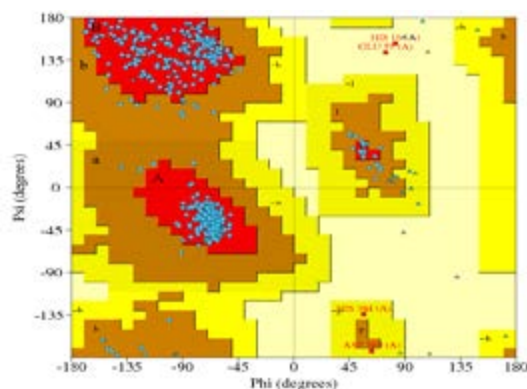


Figure 4. Ramachandran plot of the best obtained model for human cyclooxygenase-2 (COX-2).

each structure based on the contribution of both ionization states. Among the Binding Energy_{mean} values reported for the studied NSAIDs in Table 6, the minimums belong to the anions of Flurbiprofen, Ketoprofen, and Fenoprofen; which proposes a better orientation of interacting groups of these ligands within active site space. Whereas the negative charges of anions of diclofenac and meclufenamic acid, which have been highlighted in the NBO and QTAIM analyses sections, are stabilized by intramolecular hydrogen bonding, so that they could not bind as strongly to the active site of the COX-2 enzyme. The nature of these interactions is often electrostatic, hydrogen bonding, and hydrophobic interactions. As an instance, Figure 5 shows the most conventional interactions for diclofenac (in ionized and unionized states) inside the cavity of COX-2 enzyme. For unionized form, π - π interaction and hydrogen bonding contacts play a pivotal role in drug binding. Two hydrogen bonds of Ser105 and Arg106 with hydrogen and oxygen at-

oms of carboxylic acid group are essential for drug recognition. In addition, Tyr341 and phenyl group of drug constructs π - π interaction. These described interactions are also present in the ionized form. However, Arg106 involves in a stronger ionic bond with carboxylate moiety, which is more potent than the equal interaction in unionized form because of the local negative charge on this form. Therefore, the binding energy values gained for Diclofenac at the ionized state is a little more negative than the acidic state. Besides, there is a correlation between $BE_{CB}^{mean} - E_{AC}^{(2)}$ obtained by Docking calculations and $E_{AC}^{(2)}$ measured by NBO analysis of the studied NSAIDs (see Figure.6). It shows that when the geometry of a ligand lacks internal stabilization factors (i.e., intramolecular hydrogen bonding in this case), it has more tendency to interact with the active site of COX-2. Consequently, the energy released by such these interactions is more negative.

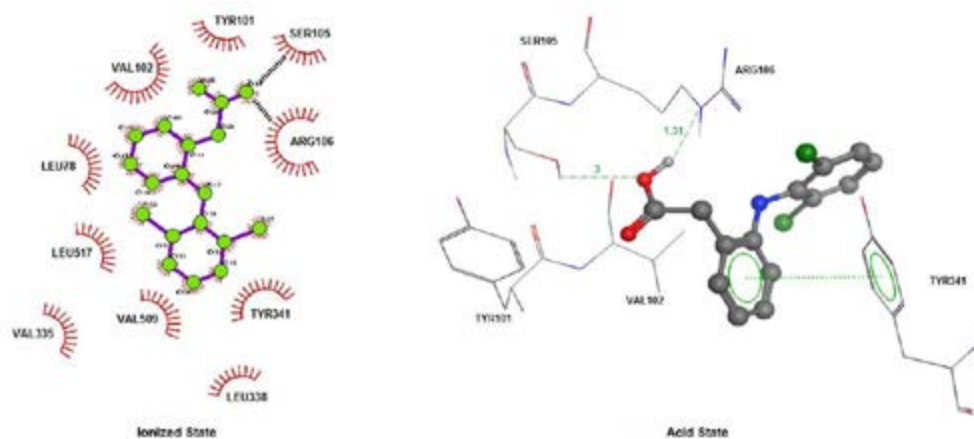


Figure 5. Interaction of diclofenac with cyclooxygenase-2 (COX-2) at different ionization states. Left (Ionized state), Right (Acid state).

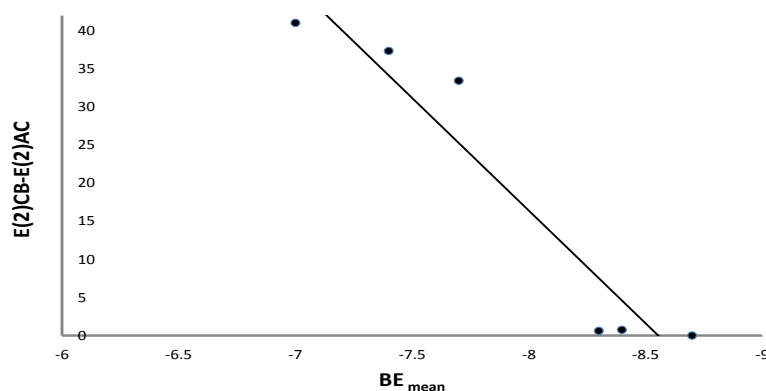


Figure 6. Correlation between the values of $E^{(2)}_{CB}-E^{(2)}_{AC}$ (kcal/mol) and BE_{mean} (kcal/mol) of the studied NSAIDs ($R^2=0.9117$).

4. Conclusion

In the present research, we investigated a detailed DFT study on the structure of some NSAIDs in the gas phase and solution. In the gas phase, acidity of the studied NSAIDs, which are able to form N-H...O intramolecular hydrogen bond during deprotonation process, is thermodynamically more favorable. The results of natural bond orbital and quantum theory of atoms in molecules analyses show stronger intramolecular hydrogen bonding between lone pairs oxygen atom ($lp(O)$) of the conjugate base and antibonding orbitals of σ^* N-H bond than C-H...O ones. Moreover, the results of QTAIM demonstrate that the hydrogen bonds are electrostatic in the nature. The calculated pK_a values of these NSAIDs in solution are very close to the experimental values. Docking study indicates that the involved active site residues are similar for both ionized and unionized states of a drug. Furthermore, computing the ionization ratio for these mentioned drugs by

considering their calculated pK_a values, substantiate the ionized form of NSAIDs as the dominant molecules in the physiological condition. Docking binding energies of the dominate molecules are a little more negative as well, especially for compounds without strong intramolecular hydrogen bonding in their structures. The findings of this investigation can be applied to gain more insight for designing novel NSAIDs and QSPR studies based on pK_a values. Also, computing the correct ionization state of a ligand will result in more accurate binding mode prediction in docking studies.

Acknowledgement

The authors are grateful to research council at Shiraz University of Medical Sciences for providing computational facilities to this work.

Conflict of Interest

None declared.

5. References

- Vane JR and Botting RM. Mechanism of Action of Nonsteroidal Anti-inflammatory Drugs. *Am J Med.* 1998;104:2-8.
- Mitchell JA, Akarasereenont P, Thiemermann C, Flower RJ, Vane JR. Selectivity of nonsteroidal antiinflammatory drugs as inhibitors of constitutive and inducible cyclooxygenase. *Proc Natl Acad Sci USA.* 1993;90:11693-7.
- Lee YT, Wang Q. Inhibition of hKv2.1, a major human neuronal voltage-gated K⁺ channel, by meclofenamic acid. *Eur J Pharmacol.* 1999;378:349-56.
- Kawamori T, Rao CV, Seibert K, Reddy BS. Chemopreventive activity of celecoxib, a specific cyclooxygenase-2 inhibitor, against colon carcinogenesis. *Cancer Res.* 1998;58:409-12.
- Hanif R, Pittas A, Feng Y, Koutsos MI, Qiao L, Staiano-Coico L, Shiff SI, Rigas B. Effects of nonsteroidal anti-inflammatory drugs on proliferation and on induction of apoptosis in colon cancer cells by a prostaglandin-independent pathway. *Biochem Pharmacol.* 1996;52:237-45.
- Kim KS, Yoon JH, Kim JK, Baek SJ, Eling TE, Lee WJ, Ryu JH, Lee JG, Lee JH, Yoo JB. Cyclooxygenase inhibitors induce apoptosis in oral

cavity cancer cells by increased expression of non-steroidal anti-inflammatory drug-activated gene. *Biochem Biophys Res Commun.* 2004;325:1298-303.

7. Weder JE, Dillon CT, Hambley TW, Kennedy BJ, Lay PA, Biffin JR, Regtop HL, Davies NM. Copper complexes of non-steroidal anti-inflammatory drugs: an opportunity yet to be realized. *Coord Chem Rev.* 2002;232:95-126.

8. Etcheverry SB, Barrio DA, Cortizo AM, Williams PAM. Three new vanadyl(IV) complexes with non-steroidal anti-inflammatory drugs (Ibuprofen, Naproxen and Tolmetin). Bioactivity on osteoblast-like cells in culture. *J Inorg Biochem.* 2002;88:94-100.

9. Sharm J, Singla AK, Dhawan S. Zinc-naproxen complex: synthesis, physicochemical and biological evaluation. *Int J Pharm.* 2003;260:217-27.

10. Moilanen E, Kankaanranta H. Tolfenamic Acid and Leukotriene Synthesis Inhibition. *Pharmacol Toxicol.* 1994;75:60-3.

11. Souza KFD, Martins JA, Pessine FBT, Custodio R. A theoretical and spectroscopic study of conformational structures of piroxicam. *Spectrochim Acta Mol Biomol Spectrosc.* 2010;75:901-7.

12. Visser SP, Ogliaro F, Sharma PK, Shaik S. What Factors Affect the Regioselectivity of Oxidation by Cytochrome P450? A DFT Study of Allylic Hydroxylation and Double Bond Epoxidation in a Model Reaction. *J Am Chem Soc.* 2002;124:11809-26.

13. Soliva R, Almansa C, Kalko SG, Luque FJ, Orozco M. Theoretical Studies on the Inhibition Mechanism of Cyclooxygenase-2. Is There a Unique Recognition Site? *J Med Chem.* 2003;46:1372-82.

14. Spartan'06 V102', Wavefunction, Inc., Irvine, CA.

15. Becke AD. Density-functional thermochemistry. III. The role of exact exchange. *J Chem Phys.* 1993;98:5648-52.

16. Lee C, Yang W, Parr R. Development of the Colle-Salvetti correlation-energy formula into a functional of the electron density. *Phys Rev B.* 1988;37:785-89.

17. Bader RFW: Atoms in Molecules: A Quantum Theory. Oxford University Press, Oxford, UK, 1990.

18. Popelier PLA: Atoms in Molecules: An Introduction. Prentice Hall, London, 2000.

19. Matta CF, Boyd RJ: The Quantum Theory of Atoms in Molecules: From Solid State to DNA and Drug Design. WILEY-VCH Verlag GmbH & Co. KGaA, Weinheim, 2007.

20. Reed AE, Curtiss LA, Weinhold F. Intermolecular interactions from a natural bond orbital, donor-acceptor viewpoint. *Chem Rev.* 1988;88:899-926.

21. Glendening ED, Badenhoop JK, Reed AE, Carpenter JE, Bohmann JA, Morales CM, Weinhold F. GEN NBO 5.0. Board of Regents of the University of Wisconsin System on behalf of the theoretical chemistry institute, Madison, 2001.

22. Bader RFW. AIM2000 Program Package, Ver. 2.0, McMaster University, Hamilton, Ontario, Canada, 2002.

23. Barone V, Cossi M, Tomasi J. A new definition of cavities for the computation of solvation free energies by the polarizable continuum model. *J Chem Phys.* 1997;107:3210-21.

24. Cammi R, Mennucci B, Tomasi J. An Attempt To Bridge the Gap between Computation and Experiment for Nonlinear Optical Properties: Macroscopic Susceptibilities in Solution. *J Phys Chem A.* 2000;104:4690-98.

25. Shokri A, Abedin A, Fattahi A, Kass SR. Effect of Hydrogen Bonds on pKa Values: Importance of Networking. *J Am Chem Soc.* 2012;134:10646-50.

26. <http://www.uniprot.org>

27. Eswar N, Eramian D, Webb B, Shen MY, Sali A. Protein structure modeling with MODELLER. *Methods Mol Bio.* 2008;426:145-59.

28. <http://www.ebi.ac.uk/thornton-srv/databases/pdbsum/Generate.html>

29. Trott O, Olson AJ. AutoDock Vina: improving the speed and accuracy of docking with a new scoring function, efficient optimization and multithreading. *J comput chem.* 2010;31:455-61.

30. Morris GM, Huey R, Olson AJ: Using AutoDock for ligand-receptor docking. *Curr Protoc Bioinformatics.* Chapter 8, 2008.

31. Humphrey W, Dalke A, Schulten K. VMD: visual molecular dynamics. *J mol graph.* 1996;14:27-38.

32. Xing D, Tan X, Chen X, Bu Y. Theoretical Study on the Gas-Phase Acidity of Multiple Sites of Cu⁺-Adenine and Cu²⁺-Adenine Complexes. *J*

Phys Chem A. 2008;112:7418-25.

33. Najdian A, Shakourian-Fard M, Fattahi A. Cooperativity effects of intramolecular OH...O interactions on pKa values of polyolalkyl sulfonic acids in the gas phase and solution: a density functional theory study. *J Phys Org Chem*. 2014;27:604-12.

34. Bader RFW. A quantum theory of molecular structure and its applications. *Chem Rev*. 1991;91:893-928.

35. Gao H, Zhang Y, Wang HJ, Liu J, Chen J. Theoretical Study on the Structure and Cation-Anion Interaction of Amino Acid Cation Based Amino Acid Ionic Liquid [Pro]⁺[NO₃]⁻. *J Phys Chem A*. 2010;114:10243-52.

36. Toth AM, Liptak MD, Phillips DL, Shields GC. Accurate relative pKa calculations for carboxylic acids using complete basis set and Gaussian-n models combined with continuum solvation methods. *J Chem Phys*. 2001;114:4595-606.

37. Kheirjou S, Abedin A, Fattahi A. Theoretical descriptors response to the calculations of the relative pKa values of some boronic acids in aqueous solution: A DFT study. *Comp Theor Chem*. 2012;1000:1-5.

38. Wynne HA, Long A, Nicholson E, Ward A, Keir D. Are altered pharmacokinetics of non-steroidal anti-inflammatory drugs (NSAIDs) a risk factor for gastrointestinal bleeding? *Br J Clin Pharmacol*. 1998;45:405-8.

39. Citra MJ. Estimating the pKa of phenols, carboxylic acids and alcohols from semi-empirical quantum chemical methods. *Chemosphere*.

1999;38:191-206.

40. Kortum G, *et al*: Dissociation Constants of Organic Acids in Aqueous Solution. IUPAC, London: Butterworth, 1961.

41. Quinteros DA, Allemandi DA, Manzo RH. Equilibrium and Release Properties of Aqueous Dispersions of Non-Steroidal Anti-Inflammatory Drugs Complexed with Polyelectrolyte Eudragit E 100. *Sci Pharm*. 2012;80:487-96.

42. Youssef AK, El-hady DA. Using of In-Situ Mercury Film Sensor Hyphenated with Affinity Voltammetry for High Throughput Drug-Protein Binding Studies. *Am. J Anal Chem*. 2013;4:159-65.

43. Fillet M, Bechet I, Piette V, Crommen J. Separation of nonsteroidal anti-inflammatory drugs by capillary electrophoresis using nonaqueous electrolytes. *Electrophoresis*. 1999;20:1907-15.

44. Bones J, Thomas K, Nesterenko PN, Paull B. On-line preconcentration of pharmaceutical residues from large volume water samples using short reversed-phase monolithic cartridges coupled to LC-UV-ESI-MS. *Talanta*. 2006;70:1117-28.

45. Muñoz de la Peña A, Mora Díez N, Bohoyo Gil D, Olivieri AC, Escandar GM. Simultaneous determination of flufenamic and meclofenamic acids in human urine samples by second-order multivariate parallel factor analysis (PARAFAC) calibration of micellar-enhanced excitation-emission fluorescence data. *Anal Chim Acta*. 2006;569:250-9.